Physica A 511 (2018) 154–165

Contents lists available at ScienceDirect

Physica A

journal homepage: www.elsevier.com/locate/physa

Cooperative fibril model: Native, amyloid-like fibril and unfolded states of proteins

J.S. Espinoza Ortiz [a,*], Cristiano L. Dias [b]

[a] Departamento de Física, Universidade Federal de Goiás, Catalão, GO 75704-020, Brazil
[b] New Jersey Institute of Technology, Department of Physics, University Heights, Newark, NJ, 07102-1982, USA

ARTICLE INFO

Article history:
Received 16 April 2018
Received in revised form 20 July 2018
Available online 26 July 2018

Keywords:
Cooperative fibril model
Native structures
Unfolded structures
Amyloid-like fibril structures
Proteins
Thermostatistics

ABSTRACT

In this paper, we start by studying the cooperative model of Hansen et al. (1998) which describes folding and unfolding transitions of proteins. Analytical expressions for different thermodynamic quantities are derived, including the degree of thermodynamic cooperativity. This model is then extended to take into account proteins that can aggregate forming amyloid-like fibril structures. Changes to the model were guided by our current understanding of the thermodynamics of fibril formation. We provide analytical equations for different thermodynamic quantities of the modified model and we study its phase diagram as a function of temperature and the binding energy of the protein to the fibril $\varepsilon^{\star}$. We find that for positive $\varepsilon^{\star}$ values, fibrils are the most stable state at low temperatures. Moreover, the model predicts that fibrils can coexist with heat unfolded, native, or cold unfolded states.

1. Introduction

The different structures adopted by proteins at various conditions of temperature and solvation determine how these biomolecules contribute to the survival of cells [1]. At physiological conditions, proteins adopt ordered conformations known as native or folded state [2,3]. The adoption of these conformations is essential for proteins to function in the cell. At conditions in which entropic effects play an important role, e.g., high temperature, the unfolded state which comprises a large number of disordered conformations is favored [4,5]. Most proteins cannot function in the cell when unfolded. Proteins can also aggregate and form amyloid-like fibril structures when subjected to the right conditions [6–8]. For some protein sequences fibril-like structures have been associated with diseases [9]. A case in point are fibrils from the amyloid-β protein which are a main constituent of plaques in the brain of patients afflicted with Alzheimer's diseases [10,11]. Thus, a same protein sequence can contribute to the survival of cells or be responsible for diseases depending on the conformations it adopts [12]. The aim of this paper is to leverage on our thermodynamic understanding of proteins to provide insights into phase diagrams that includes native, unfolded, and fibril structures—see Fig. 1.

The transition between folded and unfolded states of proteins resembles a first-order phase transition whereby order parameters describing the degree of folding change abruptly as a function of external fields, e.g., temperature. This accounts for bimodal distributions of the order parameter at the transition temperature implying that proteins spend most of their time either in the native or in the unfolded state and almost no time at intermediate conformations [13]. This type of transition is also known as cooperative and it arise when the binding energy of a "native bond" (i.e., a bond in the native state) is reinforced by the existence of other native bonds in the system [14]. This scenario for the emergence of cooperativity

* Corresponding author.
E-mail address: julio_ortiz@ufg.br (J.S. Espinoza Ortiz).

https://doi.org/10.1016/j.physa.2018.07.045
0378-4371/

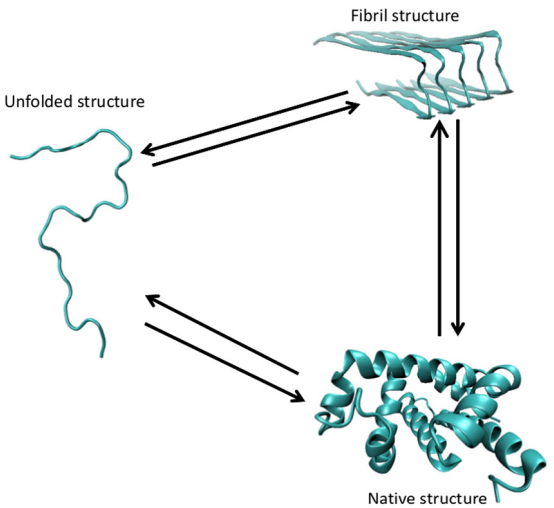

Fig. 1. Cartoon-like representation of native, unfolded and fibril structures. Arrows represent possible transitions between these states.

is consistent with the instability of many secondary structure of proteins (e.g., α-helix and β-sheet) in isolation that become stable when reinforced by non-local native contacts [15]. Thus, folding emerges from the concurrent formation of local and non-local bonds that give rise to secondary and tertiary structures of proteins, respectively [15]. However, the atomic origin of this reinforcement remains a question of debate [13]. Environmental-dependent hydrogen bonding [14], side-chain packing [16], and desolvation effects [17–19] are likely to contribute to increase folding cooperativity.

Experimentally, the degree of cooperativity of folding/unfolding transitions can be quantified using calorimetric experiments [13,20] whereby the heat capacity C_p of proteins is measured as a function of temperature [21]. These experiments have also contributed to elucidate the main molecular forces driving protein folding [15]. In particular, the intrinsic increase in heat capacity upon unfolding, i.e., $\Delta C_p = C_p^{\text{unfolded}} - C_p^{\text{native}} > 0$, is ascribed to the solvation of hydrophobic residues that are buried in the native state and become exposed to the solvent [22,23]. Accordingly the magnitude of ΔC_p was shown to increase proportionally to the number of non-polar residues in the protein [24]. This relation between ΔC_p and non-polar residues remains an important argument in favor of hydrophobic interactions being a main force driving protein folding [15,22]. Calorimetric experiments can also be used to measure changes in enthalpy ΔH_o and entropy ΔS_o at the transition temperature T_o. These quantities, i.e., ΔC_p, ΔH_o, ΔS_o, and T_o, can be used to compute changes in the Gibbs free-energy upon unfolding, i.e., $\Delta G = G^{\text{unfolded}} - G^{\text{native}}$ [21,25–28]:

$$\Delta G(T) = \Delta H_o - T\Delta S_o + \Delta C_p\left[(T - T_o) - T\ln\left(\frac{T}{T_o}\right)\right]. \tag{1}$$

The curvature of the temperature dependence of ΔG in this equation is characterized by ΔC_p. Since ΔC_p is positive for proteins, this implies that proteins undergo phase transitions (when ΔG is equal to zero) at both high and low temperatures [29,30]. As a proof of concept, hydrophobic effects incorporated in coarse-grained models of proteins were shown to reproduce these transitions [31–37]. The "cooperative model" that will be modified in this work to account for fibrillization reproduces thermodynamic properties ($\Delta C_p > 0$) of folding/unfolding transitions as well as their high degree of cooperativity [38,39].

Only recently have experiments shown that fibrils can be exist in equilibrium with dissolved proteins [40,41]. In this equilibrium, proteins dissociate and are added to the fibril reversibly [40–43]. A few experiments have measured changes in thermodynamic quantities associated with the addition/dissociation of proteins into/from a matured fibril [40,41,44]. These experiments reported both positive and negative ΔC_p [45–49]. Currently, it is unclear how the sign of ΔC_p relate to the protein sequence, the structure of fibrils, and/or solvent condition. Recent all-atom molecular dynamics simulations computed ΔC_p for the dissociation of a non-polar fragment of the Amyloid-β protein (residues 16–21) [50]. This quantity was shown to be positive as expected for the solvation of non-polar residues but small (less than 1 kJ/mol/K). The latter is consistent with the lesser sensitivity of fibrils to temperature compared to the native state. This greater stability of fibrils to temperature can be related to increased hydrogen bonding formation in these structures compared to protein folding [51]. These hydrogen bonds form cooperatively in β-sheets structures and fibrils [52]. Cooperativity in amyloid-fibrils has also been observed as a function of protein concentration. Increasing the concentration of proteins in solution accounts for a cooperative increase in the average length of fibrils [53].

This work uses the cooperative model proposed by Hansen and co-workers [38,39] to describe protein folding transitions and the realization that protein addition to fibrils may be cooperative [52]. Accordingly, in this paper we study the cooperative model of protein folding and we provide analytical expressions for the temperature dependence of its different

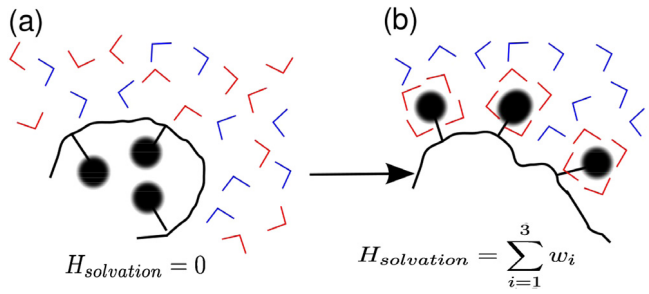

Fig. 2. Schematic representation of non-polar solvation during protein unfolding. (a) Native state wherein non-polar side chains (black circles) are buried in the dry core of the protein. (b) Unfolded state where non-polar side chains are exposed to the solvent. Water molecules surrounding non-polar side chains (red) adopt low entropic cage-like structures compared to bulk water (blue). (For interpretation of the references to color in this figure legend, the reader is referred to the web version of this article.)

thermodynamic quantities. We also compute the degree of thermodynamic cooperativity of the model that is found to be larger than for real proteins. In addition, our current understanding of the thermodynamics of fibril formation is used to modify the model to allow proteins to adopt amyloid-like fibrils. Analytical expressions for different thermodynamic quantities of the modified model are derived and its phase diagram is studied as a function of temperature and the fibril binding energy $\varepsilon^\star$. We find that for $\varepsilon^\star \geq 0$, fibrils are more stable at low temperatures. Moreover, by varying $\varepsilon^\star$, these structures can be formed from heat unfolded, native, and cold unfolded states by decreasing the temperature.

This paper is organized as follow. In Section 2 we describe the cooperative model of protein folding and its modified version in which proteins are allowed to adopt amyloid-like fibril structures. We refer to the latter as the cooperative fibril model. Next, analytical solutions and results are presented for both models in Sections 3 and 4, respectively. At last, we provide a conclusion to this work.

2. Model description

2.1. Cooperative model of protein folding

The cooperative model of Hansen et al. [38] provides insights into folding–unfolding transitions of proteins that can form N bonds in the native state. The sequence of native bonds that are formed during folding is assumed to be known and bonds are labeled according to the chronological order in which they form. The state ϕ_i of the ith bond can take values 1 or 0 dependent on whether it is formed or broken, respectively. Thus, the conformation of the protein is described by the set of ϕ_i values of its N bonds.

Based on the observation that proteins fold cooperatively, the model posits that the formation of the ith native bond will contribute to stabilize the protein structure only if bonds 1 to $i-1$ have already been formed. This is expressed mathematically in the Hamiltonian:

$$H_{\text{native}} = -\varepsilon_o \left[\phi_1 + \phi_1\phi_2 + \phi_1\phi_2\phi_3 + \cdots + \phi_1\phi_2\phi_3\cdots\phi_k\cdots\phi_N\right] . \tag{2}$$

where ε_o is the binding energy of a native bond which for simplicity is assumed to be the same for all N bonds.

Another important contribution to the energy of the system comes from solvation of non-polar amino acids that are initially buried in the dry core of the protein and become exposed to water as the protein unfolds. Non-polar solvation accounts for a reduction in the entropy of the system as water molecules prefer to adopt a reduced set of ordered (cage-like) conformations in the vicinity of non-polar molecules [31,32,54]—see Fig. 2. This effect is taken into account by a new set of variables s_i representing the state of water molecules in the vicinity of the ith native bond. Water molecules can occupy a discrete number g of states, i.e., $0 \leq s_i \leq g-1$, with equidistant energy from each other. In other words, the energy of water molecules is given by $w_i = \varepsilon_{\min} + s_i\,\Delta\varepsilon$. In the model, water states are coupled to the conformation of the protein by the Hamiltonian:

$$\begin{aligned} H_{\text{solvation}} = {} & (1-\phi_1)\,w_1 + (1-\phi_1\phi_2)\,w_2 + \cdots + (1-\phi_1\phi_2\phi_3\cdots\phi_k)\,w_k + \\ & \cdots + (1-\phi_1\phi_2\phi_3\cdots\phi_k\cdots\phi_N)\,w_N . \end{aligned} \tag{3}$$

Notice that when a new native bond is formed all the g water states associated with it contribute with the same zero energy to $H_{\text{solvation}}$—see Fig. 2. Thus, all g water states are equally likely to be adopted, e.g., the system will have a high entropy. In contrast, when the ith native bond is broken, water states defined by a large s_i will be less likely to occur than the ones defined by a small s_i. In this case, the system will have a lower entropy.

The hamiltonian defined by the sum of Eqs. (2) and (3) is known as the cooperative model for protein folding:

$$H_{\text{cooperative}} = H_{\text{native}} + H_{\text{solvation}}. \tag{4}$$

Table 1
Schematic representation of four states of a protein that can form $N = 5$ bonds. The order parameter Ψ describing these four states is shown.

Bounded sequence	Protein state	Ψ
1 1 1 1 1	Folded state	1
1 1 0 1 0	Folded/Unfolded	3/5
0 0 1 0 1	Fibril/Unfolded	2/5
0 0 0 0 0	Fibril state	0

It is defined by four parameters: N, ε_o, $\varepsilon_{\min}$, and $\Delta\varepsilon$. As shown in the result section, it accounts qualitatively for the main thermodynamic properties of folding and unfolding transitions.

2.2. Cooperative fibril model

The aim of this section is to modify the cooperative model, i.e., Eq. (4), to describe not only folding and unfolding transitions but also transitions that lead to the fibril state. For simplicity, we assume that the total number of bonds N formed by a protein in the native state is the same as the number of bonds formed in the fibril state. In the modified model, each bond ϕ_i will contribute either to the native ($\phi_i = 1$) or to the fibril ($\phi_i = 0$) state. Moreover, the formation of both native and fibril bonds will contribute to minimize the energy of the system in a cooperative manner. This can be described using a Hamiltonian that contains two terms:

$$H = H_{\text{native}} + H_{\text{fibril}}, \tag{5}$$

where H_{native} favors the native state as defined in Eq. (2) and H_{fibril} favors the fibril state. The latter can be written mathematically as:

$$\begin{aligned} H_{\text{fibril}} = & -\varepsilon^\star \left[(1-\phi_1) + (1-\phi_1)(1-\phi_2) + \cdots + \right. \\ & \left. (1-\phi_1)(1-\phi_2)\cdots(1-\phi_N)\right], \end{aligned} \tag{6}$$

where $\varepsilon^\star$ is the binding energy of a bond between the protein and the fibril. This term of the Hamiltonian is minimized whenever $\phi_i = 0$, and the protein is added to the fibril in a cooperative manner. The magnitude of $\varepsilon^\star$ as well as ε_o in Eq. (2) can increase or decrease depending on the condition of the solvent. In particular, conditions that are favorable to fibril formation are less favorable to protein folding and vice versa. This accounts for a coupling between ε_o and $\varepsilon^\star$. For simplicity we use $\varepsilon_o = (1 - \varepsilon^\star/3)$ for this coupling.

A natural order parameter to describe protein conformations that emerge from Eq. (5) is:

$$\begin{aligned} \Psi = & \frac{1}{2N}\{[\phi_1 + \phi_1\phi_2 + \cdots + \phi_1\phi_2\cdots\phi_N] - [(1-\phi_1) + (1-\phi_1)(1-\phi_2) + \\ & \cdots + (1-\phi_1)(1-\phi_2)\cdots(1-\phi_N)]\} + \frac{1}{2}, \\ = & \frac{1}{2}\Big(\langle M\rangle - \langle F\rangle\Big) + \frac{1}{2}, \end{aligned} \tag{7}$$

where $\langle M\rangle$ and $\langle F\rangle$ are the fraction of bonds in native and fibril states, respectively. Using this definition, the different protein states described by Ψ are:

$$\Psi = \begin{cases} 1, & \text{native}; \\ 1/2, & \text{unfolded}; \\ 0, & \text{fibril}. \end{cases} \tag{8}$$

Bonds of the protein that do not contribute to H_{native} or H_{fibril} are considered to be unfolded as illustrated in Table 1. Unfolded segments of the protein exhibit a high entropy, i.e., several permutations of the ϕ_i values in these segments correspond to an unfolded segment. Conversely, only specific sequences of ϕ_i, i.e., consecutive ones or consecutive zeros, account for the low entropic native and fibril states, respectively. As will be shown in the result section, under certain conditions folded and fibril states can have the same free-energy implying that these states can coexist. However, transitions of a particular protein from folded (described by sequences of ones in the model) to fibril (sequences of zero) states require it to unfold—as expected experimentally [55,56].

In addition to H_{native} and H_{fibril}, solvation of non-polar residues contribute significantly to protein folding/unfolding. This effect is taken into accounted by $H_{\text{solvation}}$ in Eq. (3). Non-polar residues are also known to play an important role accelerating the kinetics of fibril formation [57]. However, we expect the effect of these residues to play a lesser role in the thermodynamic stability of fibrils as the core of these structures are not necessarily filled with non-polar side chains [7,8]. Fibril cores can be non-polar, polar or amphiphilic depending of the amino acid sequence of the protein forming the fibril. This implies that while protein dissociation from fibrils may lead to the exposure of non-polar side chains to water this process is energetically

less important than other changes in energy, e.g., breakage of hydrogen bonds and exposure of other chemical groups of the protein to water.

Thus, we propose as a new Hamiltonian to describe a system where the protein can fold into the native state, be incorporated into a fibril, or remain unfolded:

$$H^{\star} \;=\; H_{\text{native}} + H_{\text{fibril}} + H_{\text{solvation}}\,. \tag{9}$$

This model is defined by the number of bonds N, the binding energy in the fibril state $\varepsilon^{\star}$, and solvation terms (i.e., $\varepsilon_{\min}$, $\Delta\varepsilon$, and g). The state of the system is described by two sets of variables $\{\phi_1, \phi_2, \ldots, \phi_N\}$ and $\{s_1, s_2, \ldots, s_N\}$. We refer to $H^{\star}$ as the cooperative fibril model.

3. Analytical solution

3.1. Cooperative model of protein folding

The cooperative model of protein folding has been extensively studied and analytical solutions are available in the literature [38,39]. For completeness, we show here how to compute the partition function $\mathcal{Z}$ from which meaningful physical quantities can be obtained. To compute $\mathcal{Z}$, notice that there are 2^{N-M-1} protein states with energy $-M\varepsilon_o$ for $0 < M < N-1$ and there is 1 protein state with energy $-N\varepsilon_o$. Moreover, for each protein state with energy $-M\varepsilon_o$, water molecules around the first M native bonds contribute zero energy to $H_{\text{solvation}}$. This zero energy state is g times degenerate. The other $N-M$ water states contribute to the partition function with $z_w \equiv \sum_{k=1}^{g} e^{-\beta w_k} = \left[\frac{1-e^{(g+1)\beta\Delta\varepsilon}}{1-e^{\Delta\beta\varepsilon}}\right] e^{-\beta\varepsilon_{\min}}$. The partition function is obtained by adding all these contributions together:

$$\mathcal{Z} \;=\; \sum_{M=0}^{N-1} 2^{N-M-1} e^{-M\beta\varepsilon_o} g^M \left(z_w\right)^{N-M} + e^{-N\beta\varepsilon_o} g^N. \tag{10}$$

Using $x = \frac{g}{2z_w}\, e^{\beta\varepsilon_o}$, the average energy $\langle E\rangle = -\frac{1}{\mathcal{Z}}\frac{d\mathcal{Z}}{d\beta}$ and the mean fraction of native bonds $\langle M\rangle = \frac{1}{N} x \frac{\partial \ln \mathcal{Z}}{\partial x}$ can be expressed analytically as:

$$\frac{\langle E\rangle}{N} \;=\; -\langle M\rangle\,\varepsilon_o - [1-\langle M\rangle]\,\frac{1}{z_w}\frac{\partial z_w}{\partial\beta}\,, \tag{11}$$

with

$$\langle M\rangle \;=\; \frac{\left[x^N + \frac{1}{2}\sum_{M=0}^{N-1}\frac{M}{N}x^M\right]}{\left[x^N + \frac{1}{2}\sum_{M=0}^{N-1}x^M\right]} \;=\; \frac{\left[(1-x)^2 - \frac{1}{2}\right]x^N + \frac{1}{2}x\left[\left(1-\frac{1}{N}\right)x^N + \frac{1}{N}\right]}{(1-x)\left[\left(\frac{1}{2}-x\right)x^N + \frac{1}{2}\right]}\,, \tag{12}$$

and

$$-\frac{1}{z_w}\frac{\partial z_w}{\partial\beta} \;=\; \varepsilon_{\min} + \frac{e^{-\beta\Delta\varepsilon}}{(1-e^{-\beta\Delta\varepsilon})}\left[1 - \frac{g}{z_w}e^{-\beta(\varepsilon_{\min}+(g-1)\Delta\varepsilon)}\right]\Delta\varepsilon\,. \tag{13}$$

Using these quantities, we also compute the heat capacity of the system:

$$C \;=\; d\langle E\rangle/dT. \tag{14}$$

3.2. Cooperative fibril model

The properties of a protein described by Eq. (9) can be solved analytically by computing the partition function $\mathcal{Z} = \sum e^{-\beta(H_{\text{native}}+H_{\text{fibril}}+H_{\text{solvation}})}$ of the system. β is the inverse of the thermal energy and the sum in $\mathcal{Z}$ is performed over all the possible states of the protein $\{\phi_1, \phi_2, \ldots, \phi_N\}$ and water molecules $\{s_1, s_2, \ldots, s_N\}$. To perform this sum, notice that the different energy states E of the system can be written in terms of the number of native bonds M and fibril bonds F:

$$E = \begin{cases} -(N-F)\,\varepsilon^{\star} + \displaystyle\sum_{k=1}^{N}(\varepsilon_{\min} + \Delta\varepsilon\, s_k) & \text{, for } 0 \le F \le N-1;\, M=0\,, \\ -M\varepsilon_o + \displaystyle\sum_{k=m+1}^{N}(\varepsilon_{\min} + \Delta\varepsilon s_k) & \text{; for } 1 \le M \le N-1\,, \\ -N\varepsilon_o & \text{, for } M = N\,. \end{cases} \tag{15}$$

Notice that there is only one permutation of the bond sequence (see Table 1) that accounts for an energy $-N\varepsilon_o$. In this state, water molecules around the protein contribute zero energy to $H_{\text{solvation}}$ which is g^N times degenerate. Thus, this native state contribute to $\mathcal{Z}$ with:

$$\mathcal{Z}_{\text{native}} \;=\; \exp(\beta N\varepsilon_o)\, g^N\,. \tag{16}$$

In the same vein, there are $2^{(N-M-1)}$ permutations in the bond sequence that accounts for an energy $-M\varepsilon_o$. Around the M native bonds of these permutations, water molecules do not contribute to $H_{\text{solvation}}$ which is, therefore, g^M times degenerate. The other $(N-M)$ water molecules account for a non-zero $H_{\text{solvation}}$ and they contribute to the partition function with:

$$z_w = \sum_{k=0}^{g} e^{-(\varepsilon_{\min}+k\Delta\varepsilon)} = \left[\frac{1-e^{g\beta\Delta\varepsilon}}{1-e^{\beta\Delta\varepsilon}}\right] e^{-\beta\varepsilon_{\min}} \tag{17}$$

Thus, states with M native bonds contribute to $\mathcal{Z}$ with:

$$\mathcal{Z}_M = 2^{N-M-1}\exp[\beta(N-M-1)\varepsilon_o]\, g^M\, z_w^{N-M}\,. \tag{18}$$

At last, there are $2^{(N-F-1)}$ permutations in the bond sequence with energy $-F\varepsilon^\star$. In each of these states, water molecules contribute z_w to the partition function. Thus, protein conformations that forms F bonds with the fibril will contribute to $\mathcal{Z}$ with:

$$\mathcal{Z}_F = 2^{N-F-1}\exp[\beta F\varepsilon^\star]\, z_w^N\,. \tag{19}$$

Using $x = \frac{g}{2\,z_w}\, e^{\beta\varepsilon_o^\star}$ and $y = \frac{1}{2}e^{\beta\varepsilon^\star}$, the total partition function of the system reads:

$$\begin{aligned}\mathcal{Z} &= \mathcal{Z}_F + \mathcal{Z}_M + \mathcal{Z}_{\text{native}}\,,\\ &= (2z_w)^N\left\{\left[y^N + \frac{1}{2}\sum_{F=0}^{N-2} y^{N-F-1}\right] + \left[\frac{1}{2}\sum_{M=1}^{N-1} x^M + x^N\right]\right\}.\end{aligned} \tag{20}$$

From the partition function, we can compute the mean fraction of native bonds $\langle M\rangle$, the mean fraction of bonds in the fibril state $\langle F\rangle$, and the mean energy of the system $\langle E\rangle$,

$$\begin{aligned}\langle M\rangle &= \frac{\left(\frac{1}{2}+x^2\right)x^N - \frac{1}{2}x\left[\left(3+\frac{1}{N}\right)x^N - \frac{1}{N}\right]}{\left[\left(\frac{1}{2}-x\right)x^N + \frac{1}{2}x\right](1-y) + \left[\left(\frac{1}{2}-y\right)y^N + \frac{1}{2}y\right](1-x)}\,\frac{(1-y)}{(1-x)}\,,\\ \langle F\rangle &= \frac{\left(\frac{1}{2}+y^2\right)y^N - \frac{1}{2}y\left[\left(3+\frac{1}{N}\right)y^N - \frac{1}{N}\right]}{\left[\left(\frac{1}{2}-x\right)x^N + \frac{1}{2}x\right](1-y) + \left[\left(\frac{1}{2}-y\right)y^N + \frac{1}{2}y\right](1-x)}\,\frac{(1-x)}{(1-y)}\,,\end{aligned} \tag{21}$$

and

$$\frac{\langle E\rangle}{N} = -\langle M\rangle\varepsilon_o - [1-\langle M\rangle]\,\frac{1}{z_w}\frac{dz_w}{d\beta} - \langle F\rangle\,\varepsilon^\star\,. \tag{22}$$

The free-energy of the system $\mathcal{F} = -T\ln(\mathcal{Z})$ and the entropic energy $-TS = \mathcal{F} - \langle E\rangle$ are also readily available from the partition function. An analytical expression for the heat capacity is provided in Appendix.

4. Results and discussion

4.1. Cooperative model of protein folding

The original cooperative model of protein folding described by Eq. (4) provides important insights into the thermodynamic properties of this transitions. These insights are summarized in Fig. 3. In panel a, we show the mean fraction of native bonds $\langle M\rangle$ (given by Eq. (12)) as a function of temperature. This figure indicates that the native state of the protein (when $\langle M\rangle$ is close to 1) is only stable at intermediate temperatures and it unfolds at both high and low temperatures. These transitions are known as heat and cold denaturation, respectively [29,31]. They emerge from the temperature dependence of free energy difference between folded $\mathcal{F}_f$ and unfolded $\mathcal{F}_u$ states, i.e., $\Delta\mathcal{F} = \mathcal{F}_u - \mathcal{F}_f$. This quantity can be computed from the partition function at folded, i.e., $\mathcal{Z}_f = \left(g\, e^{\beta\varepsilon_o}\right)^N$, and unfolded, i.e., $\mathcal{Z}_u = (2\,z_w)^N$, states: $\Delta\mathcal{F}/N = -T\ln(\mathcal{Z}_u/\mathcal{Z}_f) = \varepsilon_o - T\ln\left(2\,\frac{z_w}{g}\right)$. This free energy difference is depicted by a black line in Fig. 3b. Folded and unfolded states are stable whenever $\Delta\mathcal{F}$ is positive and negative, respectively. Coexistence between these states are characterized by $\Delta\mathcal{F} = 0$ and they occur at both high and low temperatures.

In Fig. 3b we also show the difference in internal energy between folded and unfolded states $\langle\Delta E\rangle/N = \left(E_u - E_f\right)/N = \left(\varepsilon_o - \frac{1}{z_w}\frac{dz_w}{d\beta}\right)$ as well as the difference in entropic energy between folded and unfolded states $-T\,\Delta S/N = -T\left(S_u - S_f\right)/N = \Delta\mathcal{F}/N - \langle\Delta E\rangle/N$ as a function of temperature. At high temperature, i.e., $T > 4$ in Fig. 3b, both $\Delta\mathcal{F}$ and $-T\Delta S$ are negative while $\langle\Delta E\rangle$ is positive. This implies that the free-energy of the unfolded state is dominated by entropy while it is opposed by $\langle\Delta E\rangle$. This entropic contribution can be ascribed to the increased number of states of the unfolded protein given by H_{native}. In contrast, protein unfolding at low temperature is dominated by enthalpy and this can be ascribed to ordering of water molecules around non-polar residues given by $H_{\text{solvation}}$.

In Fig. 3c, we show the dependence of C (see Eq. (14)) on temperature. C peaks at both high and low temperatures characterizing heat and cold denaturation, respectively. An important feature of C is that its magnitude is smaller in the

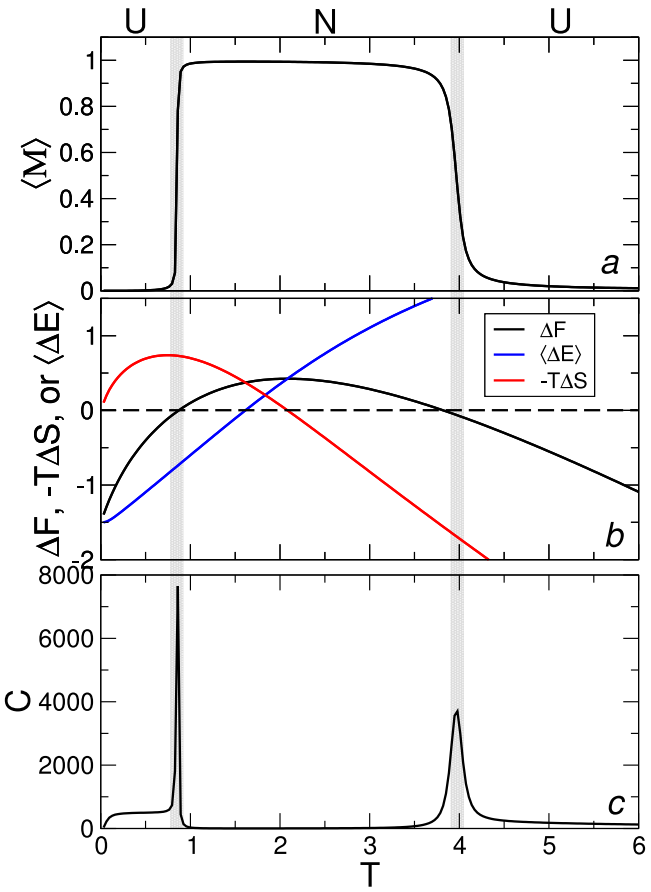

Fig. 3. Cooperative model of protein folding. Temperature dependence of (a) the fraction of native bonds ($\langle M\rangle$), (b) changes in internal energy ($\langle \Delta E\rangle$), entropic energy ($-T\Delta S$) as well as free-energy ($\Delta \mathcal{F}$) upon unfolding, and (c) heat capacity C. Shaded areas highlight folding and unfolding transitions. Native and unfolded states are represented by the letters N and U. We used $N = 500$, $\varepsilon_o = 1$, $\varepsilon_{\min} = -2.5$, $\Delta\varepsilon = 0.207$ and $g = 53$.

native state compared to the unfolded state at both heat and cold denaturations. This accounts for a positive change in heat capacity upon unfolding $\Delta C = C_u - C_f$. The rational behind this change is ascribed to the exposure of non-polar residues to water upon unfolding that accounts a large increase in heat capacity [58]. This is consistent with the linear dependence of ΔC on the number of non-polar residues that was observed for various proteins [24].

In Fig. 4a we show ΔC upon heat denaturation. The peak in the heat capacity can be used to estimate the degree of thermodynamic cooperativity of folding/unfolding transitions by comparing van't Hoff and calorimetric enthalpies [20]. The van't Hoff enthalpy is given as $\Delta H_{\rm vH} = 2T_{\max}\sqrt{k_{\rm b}C_{\max}}$ where $C_{\max}$ and $T_{\max}$ are the peak in the heat capacity value and the transition temperature as shown in Fig. 4b. The calorimetric enthalpy is computed by integrating the heat capacity across the transition region $\Delta H_{\rm cal} = \int C_{\rm b} dT$ where $C_{\rm b}$ is the heat capacity after proper subtraction of the baseline—see Fig. 4. The ratio of these quantities, i.e.,

$$\Delta H_{\rm vH}/\Delta H_{\rm cal} = \kappa_2 \equiv \frac{2T_{\max}\sqrt{k_{\rm b}C_{\max}}}{\Delta H_{\rm cal}}, \tag{23}$$

provides an estimate of how distributions of enthalpies at folded and unfolded states are separated at the coexistence temperature. κ_2 is approximately unity for many real systems accounting for bimodal distributions of enthalpy at the coexistence temperature [20]. For the cooperative model of protein folding and the parameters used to generate Fig. 4, we find that $\kappa_2 \approx 10$. Large values of κ_2, i.e., $\kappa_2 \gg 1$, are expected to emerge from the functional form of $H_{\rm native}$ independently of model parameters.

4.2. Cooperative fibril model

The phase diagram of the cooperative fibril model is depicted in Fig. 5. Colors in this diagram represent the order parameter Ψ which is shown as a function of temperature and the fibril binding energy $\varepsilon^\star$. Transitions between the different

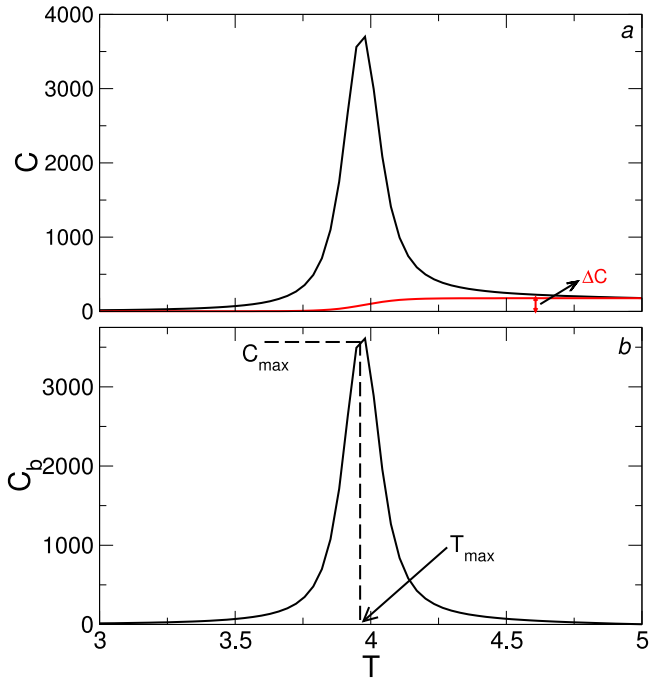

Fig. 4. Cooperative model of protein folding. (a) Temperature dependence of the heat capacity C around heat denaturation. The baseline (red line) given by $7 \times 10^{-5}/(1 + \exp(-15(T - 3.978))) + 1 \times 10^{-5}$ is shown as well as ΔC. (b) Heat capacity after baseline subtraction. $C_{\max} = 3698.7$ and $T_{\max} = 3.978$ are also shown. Data are for $N = 500$, $\varepsilon_o = 1$, $\varepsilon_{\min} = -2.5$, $\Delta\varepsilon = 0.207$ and $g = 53$. (For interpretation of the references to color in this figure legend, the reader is referred to the web version of this article.)

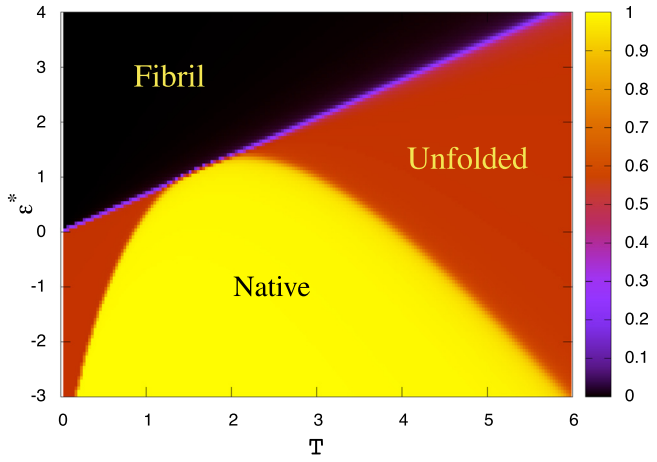

Fig. 5. Phase diagram of the cooperative fibril model. The color scheme represents the order parameter Ψ which is shown as a function of temperature and the fibril binding energy $\varepsilon^\star$. The fibril state ($\Psi = 0$) is represented in black, the unfolded state ($\Psi = 0.5$) is depicted in red and the folded state ($\Psi = 1$) is shown in yellow. Data are for $N = 500$, $\varepsilon_{\min} = -2.5$, $\Delta\varepsilon = 0.207$ and $g = 53$. Notice that we are using $\varepsilon_o = 1 - \varepsilon^\star/3$ for the coupling between ε_o and $\varepsilon^\star$ (see Model Description). (For interpretation of the references to color in this figure legend, the reader is referred to the web version of this article.)

phases occur within a short range of temperatures and $\varepsilon^\star$ values which is the signature of thermodynamic cooperativity. Native and fibril conformations in the model exhibit low energy and, therefore, they are singled out at low temperatures. Similarly, the $H_{\text{solvation}}$ term in Eq. (3) accounts for an unfolded state that has a low energy (lower than the energy of the native state) at very low temperatures. Competition between these energetic terms provides the rational for the low temperature behavior in Fig. 5. The behavior of the phase diagram at high temperature is determined by entropy which is higher for the unfolded state.

To highlight the complexity of the phase diagram of the cooperative fibril model, we show in Fig. 6 the dependence of Ψ (upper panels) and heat capacity (bottom panels) on temperature. These quantities were computed from Eqs. (7) and (A.1).

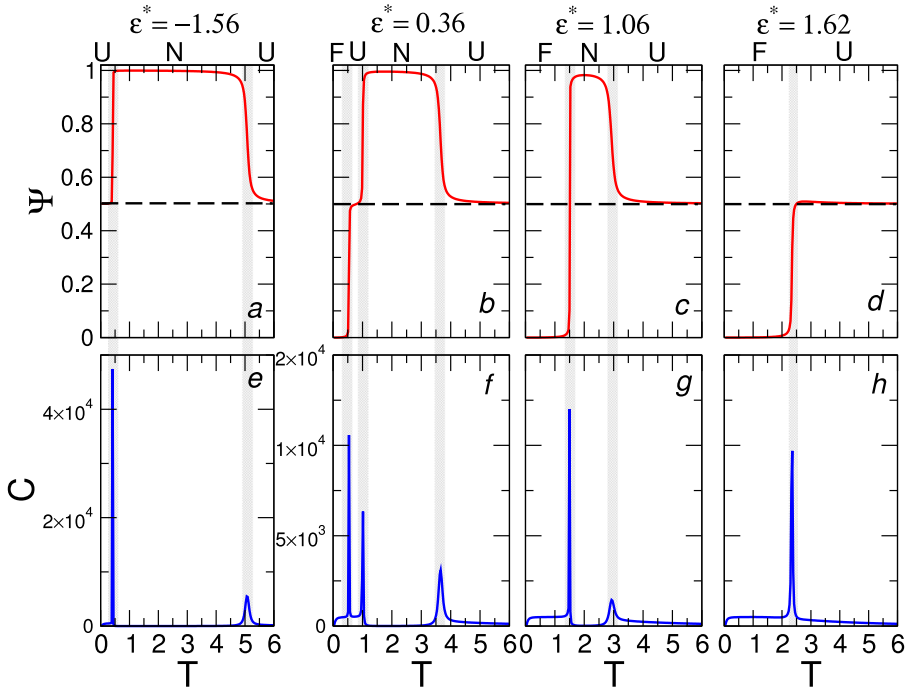

Fig. 6. Cooperative fibril model. Temperature dependence of (a–d) the order parameter Ψ and (e–h) the heat capacity. Columns from left to right correspond to $\varepsilon^\star = -1.56$, 0.36, 1.06, and 1.62, respectively. Unfolded, native, and fibril states are represented by letters U, N, and F. Shaded areas highlight temperature regions for which there is a phase transition. Data are for $N = 500$, $\varepsilon_{\min} = -2.5$, $\Delta\varepsilon = 0.207$ and $g = 53$.

For $\varepsilon^\star = -1.56$ (panels *a* and *e*), the protein undergoes two phase transitions: heat and cold denaturations. This behavior is similar to the one in the original cooperative model (see Section 4.1) where fibrils are non existent. In this case, the protein unfolds ($\Psi = 1/2$) at both low and high temperatures and the native state is stable at intermediate temperatures when $\Psi = 1$ in panel *a*. These transitions are characterized by peaks in the heat capacity in panel *e*. For $\varepsilon^\star = 0.36$ (panels *b* and *f*), in addition to heat and cold denaturation, the protein also forms fibrils at low temperature. Accordingly, the order parameter exhibits plateau regions at $\Psi = 1$, 0.5, and 0, whereas the heat capacity peaks at the three values of temperature where Ψ changes. Notice that for this $\varepsilon^\star$ value, fibrillization emerges from the cold unfolded state. The two transitions that emerge for $\varepsilon^\star = 1.06$ (panels *c* and *g*) are heat denaturation and fibrillization from the native state. Peaks in the heat capacity associated with this transition are shown in panel *g*. At last, panels *d* and *h* show fibrillization emerging from the unfolded stated for $\varepsilon^\star = 1.62$ and its corresponding peak in the heat capacity.

Fig. 6 predicts that for some parameters of the model, fibrils can form from cold unfolded, native, or heat unfolded states. Experimentally, equilibrium properties of fibrils are studied when these structures exist in equilibrium with unfolded proteins (mostly at ambient temperature) [40]. However, tuning the content of secondary structures of a small peptide (from mostly α-helix to mostly β-sheet) did not prevent fibrillization [56]. This suggests that the formation of fibrils is robust and it does not depend significantly on the structure of the protein that is being added to it. Our results are consistent with these experimental findings inasmuch as fibrils can form from different structures.

Another result that emerges from the model is that fibrils may exist in equilibrium with native protein structures close to the fibrillization transition in Fig. 6 *c* and *g*. Coexistence between these two states is possible whenever the energy in the fibril state is close to the energy in the native state, i.e., $\varepsilon^\star \approx \varepsilon_o$. Thus, for the coupling between $\varepsilon^\star$ and ε_o used in this work (i.e., $\varepsilon_o = 1 - \varepsilon^\star/3$), coexistence between native an fibril states will emerge close to $\varepsilon^\star = \varepsilon_o = 0.75$. In Fig. 7, we show the order parameter Ψ and the heat capacity for $\varepsilon^\star$ values close to 0.75, i.e., 0.70 (panels *a* and *d*), 0.80 (panels *b* and *e*), and 0.85 (panels *c* and *f*). The temperature range $\Delta T^\star$ in which the unfolded state is stable becomes shorter as $\varepsilon^\star$ increases from 0.7 to 0.8, and it is zero at 0.85 when the unfolded state is not an equilibrium state. Notice that for a general coupling of the form $\varepsilon_o = 1 - A\varepsilon^\star$ with $A > 0$, coexistence between native and fibril states will occur when $\varepsilon_o = \varepsilon^\star = 1/(1 + A)$. One may speculate that under such conditions of $\varepsilon^\star$ and at the transition temperature, fibrils may be less toxic (i.e., they might be more inert) as proteins in the solution may still exert their biological function.

5. Conclusion

In this paper we have studied the cooperative model of folding/unfolding transitions of proteins. We obtained analytical expressions for various thermodynamic quantities as a function of temperature and we showed that the model exhibits a

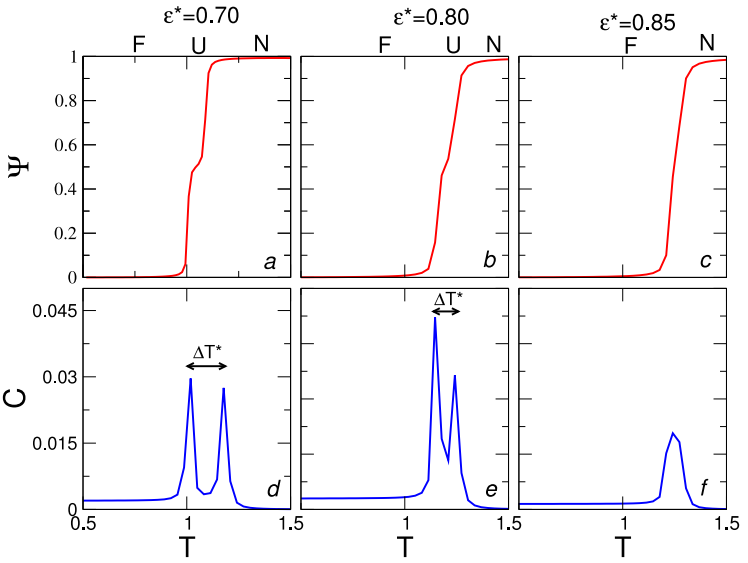

Fig. 7. Coexistence between fibril and native structures for the cooperative fibril model. Temperature dependence of (a–c) the order parameter Ψ and (d–f) the heat capacity. Columns from left to right correspond to $\varepsilon^\star = 0.70, 0.80$ and 0.85, respectively. Fibril, unfolded and native states are represented by letters F, U and N. Notice that as $\varepsilon^\star$ increases, the temperature range $\Delta T^\star$ in which the unfolded state is stable becomes shorter. Data are for $N = 500$, $\varepsilon_{\min} = -2.5$, $\Delta\varepsilon = 0.207$ and $g = 53$.

degree of thermodynamic cooperativity that is larger than for real proteins. Changes in the functional form of the Hamiltonian may be needed to account for a degree of cooperativity that resembles more closely experimental data. In addition, we modified the cooperative model to take into account amyloid-like fibrils. In this process, our current understanding of the thermodynamic properties of amyloid fibrils was taken into account. The modified model was studied as a function of temperature and the fibril binding energy $\varepsilon^\star$. The modified model incorporates a natural order parameter to describe unfolded, fibril and folded states. Moreover, the model is exact in as much as the partition function and thermodynamic quantities can be derived analytically. We find that for $\varepsilon^\star \geq 0$, fibrils are the most stable state at low temperatures. Moreover, by varying $\varepsilon^\star$, these structures can form from heat unfolded, native, and cold unfolded states by decreasing the temperature.

Acknowledgments

CLD would like to thank Alex Hansen for motivating this work and Markus Miettienen for insightful discussions. JSEO would like to thank NJIT for its kind hospitality during his visits to the Department of Physics where part of this work was developed. This work was supported by the Goiás State Research Foundation - FAPEG .

Appendix. Analytic calculations

We focus on the cooperative fibril model developed in Section 2.2, to provide an expression for its heat capacity C:

$$\begin{aligned}\frac{1}{N^2}T^2C &= \frac{1}{N^2}\frac{d^2\ln\mathcal{Z}}{d\beta^2}, \\ &= \frac{1}{N}\frac{\partial\langle M\rangle}{\partial\beta}\left(\varepsilon_o - \frac{1}{z_w}\frac{\partial z_w}{\partial\beta}\right) + [1-\langle M\rangle]\frac{1}{N}\frac{\partial}{\partial\beta}\left(\frac{1}{z_w}\frac{\partial z_w}{\partial\beta}\right) + \frac{1}{N}\frac{\partial\langle F\rangle}{\partial\beta},\end{aligned} \tag{A.1}$$

where $\langle M\rangle$ and $\langle F\rangle$ are the fraction of bonds in the native and fibril states, respectively. To compute these quantities and their derivatives, we define:

$$\begin{aligned} q_x &= (\frac{1}{2}-x)x^N + \frac{1}{2}x, \qquad & q_y &= (\frac{1}{2}-y)y^N + \frac{1}{2}y, \\ q &= (1-y)\,q_x + (1-x)\,q_y, \end{aligned} \tag{A.2}$$

and

$$\begin{aligned} p_x &= (\tfrac{1}{2}+x^2)x^N - \tfrac{1}{2}\left[(3+\tfrac{1}{N})x^N - \tfrac{1}{N}\right]x, \\ p_y &= (\tfrac{1}{2}+y^2)y^N - \tfrac{1}{2}\left[(3+\tfrac{1}{N})y^N - \tfrac{1}{N}\right]y. \end{aligned} \tag{A.3}$$

In term of these variables, $\langle M\rangle$ and $\langle F\rangle$ can be written:

$$\langle M\rangle = \frac{p_x}{q}\frac{(1-y)}{(1-x)} \quad , \quad \langle F\rangle = \frac{p_y}{q}\frac{(1-x)}{(1-y)}\,, \tag{A.4}$$

and their derivatives read,

$$\begin{aligned}\frac{1}{\langle M\rangle}\frac{\partial\langle M\rangle}{\partial\beta} &= \left\{\left[\frac{x}{(1-x)}+\frac{x}{p_x}\frac{dp_x}{dx}-\frac{x}{q}\frac{\partial q}{\partial x}\right]\left(\varepsilon_o-\frac{1}{z_w}\frac{dz_w}{d\beta}\right)-\left[\frac{y}{(1-y)}-\frac{yq_x}{q}\right]\varepsilon^\star\right\}\,,\\ \frac{1}{\langle F\rangle}\frac{\partial\langle F\rangle}{\partial\beta} &= \left\{\left[\frac{y}{(1-y)}+\frac{y}{p_y}\frac{dp_y}{dy}-\frac{y}{q}\frac{\partial q}{\partial y}\right]\varepsilon^\star-\left[\frac{x}{(1-x)}-\frac{xq_y}{q}\right]\left(\varepsilon_o-\frac{1}{z_w}\frac{dz_w}{d\beta}\right)\right\}\,.\end{aligned} \tag{A.5}$$

At last, we define $r = e^{-\beta\triangle\varepsilon}$, with $\beta = \frac{1}{T}$, to compute from Eq. (17) the following quantities:

$$\begin{aligned}-\frac{1}{z_w}\frac{\partial z_w}{\partial\beta} &= \varepsilon_{\min}+\left[\frac{r}{1-r}-g\,\frac{r^g}{1-r^g}\right]\triangle\varepsilon\,,\\ \frac{\partial}{\partial\beta}\left(\frac{1}{z_w}\frac{\partial z_w}{\partial\beta}\right) &= \left[\frac{r}{(1-r)^2}-g^2\frac{r^g}{(1-r^g)^2}\right](\triangle\varepsilon)^2\,.\end{aligned} \tag{A.6}$$

Establishing that the coupling between ε_o and $\varepsilon^\star$ is given by $\varepsilon_o = 1-\varepsilon^\star/3$, the heat capacity C can now be computed by replacing Eqs. (A.4)–(A.6) into Eq. (A.1).

References

[1] C. Branden, J. Tooze, Introduction to Protein Structure, second ed., Garland Publishing Inc., 1999.
[2] M.F. Perutz, M.G. Rossmann, A.F. Cullis, H. Muirhead, G. Will, Structure of hæmoglobin: a three-dimensional fourier synthesis at 5.5-å. resolution, obtained by x-ray analysis, Nature 185 (1960) 416–422.
[3] C.B. Anfinsen, Principles that govern the folding of protein chains, Science 181 (1973) 223.
[4] H. Wu, Studies on denaturation of proteins. 13. a theory of denaturation, Chin. J. Physiol. 5 (1931) 321–344.
[5] H. Wu, Studies on denaturation of proteins xiii. a theory of denaturation, Adv. Protein Chem. 46 (1995) 6–26.
[6] F. Chiti, C.M. Dobson, Protein misfolding, functional amyloid, and human disease, Annu. Rev. Biochem. 75 (2006) 333.
[7] M. Fändrich, M.A. Fletcher, C.M. Dobson, Amyloid fibrils from muscle myoglobin, Nature 410 (6825) (2001) 165.
[8] M. Fändrich, M. Dobson, Christopher, The behaviour of polyamino acids reveals an inverse side chain effect in amyloid structure formation, EMBO J. 21 (2002) 5682.
[9] J. Hardy, G. Higgins, Alzheimer's disease: the amyloid cascade hypothesis, Science 256 (1992) 184.
[10] E.D. Roberson, L. Mucke, 100 years and counting: Prospects for defeating alzheimer's disease, Science 314 (2006) 781.
[11] I. Hamley, The amyloid beta peptide: a chemist's perspective. role in alzheimer's and fibrillization, Chem. Rev. 112 (10) (2012) 5147–5192.
[12] C.M. Dobson, Protein folding and misfolding, Nature 426 (2003) 884.
[13] H. Chan, Z. Zhang, S. Wallin, Z. Liu, Cooperativity, local-nonlocal coupling, and nonnative interactions: Principles of protein folding from coarse-grained models, Ann. Rev. Phys. Chem. 62 (2011) 301.
[14] H. Kaya, H.S. Chan, Energetic components of cooperative protein folding, Phys. Rev. Lett. 85 (22) (2000) 4823.
[15] K. Dill, Dominant forces in protein folding, Biochemistry 29 (1990) 7133.
[16] K.A. Dill, S.B. Ozkan, M.S. Shell, T.R. Weikl, The protein folding problem, Ann. Rev. Biohys. 37 (2008) 289.
[17] M.S. Cheung, A.E. García, J.N. Onuchic, Protein folding mediated by solvation: water expulsion and formation of the hydrophobic core occur after the structural collapse, Proc. Natl. Acad. Sci. USA 99 (2) (2002) 685–690.
[18] Y. Levy, J.N. Onuchic, Water mediation in protein folding and molecular recognition, Annu. Rev. Biophys. Biomol. Struct. 35 (2006) 389–415.
[19] Z. Liu, H.S. Chan, Solvation and desolvation effects in protein folding: native flexibility, kinetic cooperativity and enthalpic barriers under isostability conditions, Phys. Biol. 2 (4) (2005) S75.
[20] H. Kaya, H.S. Chan, Polymer principles of protein calorimetric two-state cooperativity, Proteins: Struct. Funct. Bioinf. 40 (4) (2000) 637–661.
[21] P.L. Privalov, Thermodynamics of protein folding, J. Chem. Thermodyn. 29 (1997) 447–474.
[22] W. Kauzmann, Some factors in the interpretation of protein denaturation, Adv. Protein Chem. 14 (1959) 1.
[23] C.L. Dias, T. Hynninen, T. Ala-Nissila, A.S. Foster, M. Karttunen, Hydrophobicity within the three-dimensional mercedes-benz model: Potential of mean force, J. Chem. Phys. 134 (2011) 65106.
[24] A.D. Robertson, K.P. Murphy, Protein structure and the energetics of protein stability, Chem. Rev. 97 (5) (1997) 1251–1268.
[25] C.L. Dias, T. Ala-Nissila, J. Wong-ekkabut, I. Vattulainen, M. Grant, M. Karttunen, The hydrophobic effect and its role in cold denaturation, Cryobiology 60 (2010) 91–99.
[26] L. Smeller, Pressure-temperature phase diagrams of biomolecules, Biochim. Biophys. Acta - Protein Struct. Mol. Enzymol. 1595 (2002) 11–29.
[27] A. Zipp, W. Kauzmann, Pressure denaturation of metmyoglobin, Biochemistry 12 (1973) 4217–4228.
[28] S.A. Hawley, Reversible pressure-temperature denaturation of chymotrypsinogen, Biochemistry 10 (1971) 2436–2442.
[29] P.L. Privalov, Y.V. Griko, S.Y. Venyaminov, Cold denaturation of myoglobin, J. Mol. Biol. 190 (1986) 487–498.
[30] P.L. Privalov, Cold denaturation of protein, Crit. Rev. Biochem. Mol. Biol. 25 (4) (1990) 281.
[31] C.L. Dias, T. Ala-Nissila, M. Karttunen, I. Vattulainen, M. Grant, Microscopic mechanism for cold denaturation, Phys. Rev. Lett. 100 (2008) 118101–118105.
[32] C.L. Dias, Unifying microscopic mechanism for pressure and cold denaturations of proteins, Phys. Rev. Lett. 109 (2012) 048104–048109.
[33] P.D.L. Rios, G. Caldarelli, Putting proteins back into water, Phys. Rev. E 62 (2000) 8449.
[34] P.D.L. Rios, G. Caldarelli, Cold and warm swelling of hydrophobic polymers, Phys. Rev. E 63 (2001) 031802.
[35] M.I. Marques, J.M. Borreguero, H.E. Stanley, N.V. Dokholyan, Possible mechanism for cold denaturation of proteins at high pressure, Phys. Rev. Lett. 91 (13) (2003) 138103.
[36] P. Das, S. Matysiak, Direct characterization of hydrophobic hydration during cold and pressure denaturation, J. Phys. Chem. B 116 (18) (2012) 5342–5348.
[37] B.A. Patel, P.G. Debenedetti, F.H. Stillinger, P.J. Rossky, A water-explicit lattice model of heat, cold, and pressure induced protein unfolding, Biophys. J. 93 (2007) 4116.

[38] A. Hansen, M.H. Jensen, K. Sneppen, G. Zocchi, Statistical mechanics of warm and cold unfolding in proteins, Eur. Phys. J. B 6 (1) (1998) 157–161.
[39] A. Bakk, J.S. Høye, A. Hansen, K. Sneppen, M.H. Jensen, Pathways in two-state protein folding, Biophys. J. 79 (5) (2000) 2722–2727.
[40] R. Wetzel, Kinetics and thermodynamics of amyloid fibril assembly, Acc. Chem. Res. 39 (9) (2006) 671–679.
[41] B. O'Nuallain, S. Shivaprasad, I. Kheterpal, R. Wetzel, Thermodynamics of a_β(1-40) amyloid fibril elongation, Biochemistry 44 (2005) 12709.
[42] T. Urbic, S. Najem, C.L. Dias, Thermodynamic properties of amyloid fibrils in equilibrium, Biophys. Chem. 231 (2017) 155–160.
[43] L.G. Rizzi, S. Auer, Amyloid fibril solubility, J Phys. Chem. B 119 (2015) 14631–14636.
[44] R. Wetzel, Physical chemistry of polyglutamine: Intriguing tales of a monotonous sequence, J. Mol. Biol. 421 (4–5) (2012) 466–490.
[45] T. Ikenoue, Y.-H. Lee, J. Kardos, M. Saiki, H. Yagi, Y. Kawata, Y. Goto, Cold denaturation of alpha-synuclein amyloid fibrils, Angew. Chem. Int. Ed. 53 (2014) 7799–7804.
[46] J. Kardos, K. Yamamoto, K. Hasegawa, H. Naiki, Y. Goto, Direct measurement of the thermodynamic parameters of amyloid formation by isothermal titration calorimetry, J. Biol. Chem. 279 (53) (2004) 55308–55314.
[47] M.D. Jeppesen, K. Hein, P. Nissen, P. Westh, D.E. Otzen, A thermodynamic analysis of fibrillar polymorphism, Biophys. Chem. 149 (1) (2010) 40–46.
[48] B. Morel, L. Varela, F. Conejero-Lara, The thermodynamic stability of amyloid fibrils studied by differential scanning calorimetry, J. Phys. Chem. B 114 (11) (2010) 4010–4019.
[49] T. Ikenoue, Y.-H. Lee, J. Kardos, H. Yagi, T. Ikegami, H. Naiki, Y. Goto, Heat of supersaturation-limited amyloid burst directly monitored by isothermal titration calorimetry, Proc. Natl. Acad. Sci. 111 (18) (2014) 6654–6659.
[50] S.R. Jampani, F. Mahmoudinobar, Z. Su, C. Dias, Thermodynamics of aβ16-21 dissociation from a fibril: Enthalpy, entropy, and volumetric properties, Proteins: Struct. Funct. Bioinf. 83 (2015) 19.
[51] A.W. Fitzpatrick, T.P.J. Knowles, C.A. Waudby, M. Vendruscolo, C.M. Dobson, Inversion of the balance between hydrophobic and hydrogen bonding interactions in protein folding and aggregation, PLoS Comput. Biol. 7 (2011) e10002169.
[52] Y.-L. Zhao, Y.-D. Wu, A theoretical study of β-sheet models? is the formation of hydrogen-bond networks cooperative? J. Am. Chem. Soc. 124 (8) (2002) 1570–1571.
[53] M.E. Van Raaij, J. Van Gestel, I.M. Segers-Nolten, S.W. De Leeuw, V. Subramaniam, Concentration dependence of α-synuclein fibril length assessed by quantitative atomic force microscopy and statistical–mechanical theory, Biophys. J. 95 (10) (2008) 4871–4878.
[54] H.S. Frank, M.W. Evans, Free volume and entropy in condensed systems iii, entropy in binary liquid mixtures; partial molal entropy in dilute solutions; structure and thermodynamics in aqueous electrolytes, J. Chem. Phys. 13 (1945) 507.
[55] M. Fändrich, a.B.K. Forge, Vincent, M. Kittler, C.M. Dobson, S. Diekmann, Myoglobin forms amyloid fibrils by association of unfolded polypeptide segments, Proc. Natl. Acad. Sci. USA 100 (2003) 15463.
[56] M. Calamai, F. Chiti, C.M. Dobson, Amyloid fibril formation can proceed from different conformations of a partially unfolded protein, Biophys. J. 89 (6) (2005) 4201–4210.
[57] F. Chiti, M. Stefani, N. Taddei, G. Ramponi, C.M. Dobson, Rationalization of the effects of mutations on peptide andprotein aggregation rates, Nature 424 (6950) (2003) 805.
[58] J.T. Edsall, Apparent molal heat capacities of amino acids and other organic compounds, J. Am. Chem. Soc. 54 (1935) 1506–1507.